Experimental analysis of a medium-scale tandem flapping wing system

Thomas Lambert* and Grigorios Dimitriadis†
University of Liège, 4000 Liège, Belgium

The present research concerns the design and wind tunnel testing of a medium-scale tandem flapping wing setup. As first step, tests were conducted with simple wings (rectangular flat plates at 0° of pitch). This provided a basic understanding of the key parameters for these types of flows as well as a general understanding of the aerodynamic response. A first series of tests focused on the semi-flapping case, where only the front wing was flapping, while the aft one remained at a fixed dihedral angle. It was found that the front wing's lift was heavily degraded when the aft wing's dihedral was important. The aft wing was also shown to generate thrust in all situations evaluated. For tandem flapping situations, the phase offset between the two sets of wings revealed to be a critical factor in the aerodynamic response. Finally, it was shown that increasing the horizontal distance between the two sets of wings lead to a significant decrease in the mean lift produced by both sets; and most notably by the front one.

I. Introduction

With recent advances in micro-electronics, battery technologies and the miniaturization of high performance brushless motors, it is now easier than ever to build and fly flapping drones. Over the years, the complexity of such systems has increased significantly. Currently, research efforts focus on the down-sizing of components and the development of micro-scale, high frequency systems (entomopters, hummingbirds) [1–5]. Due to their small size and weight, such setups are bound to low Reynolds numbers. Although higher Reynolds flappers [6–8] have been built, they are often limited to low *reduced* frequency due to energy and structural constraints. Currently, most applications concern only single wing flapping systems. Multi-wings systems, while repeatedly found in nature, are often neglected. The little work being done on such setups focuses on very small dimensions (dragonfly-like); and almost nothing is being done for medium-scale systems.

Thanks to advances in motor technology and manufacturing processes, it is now possible to study the impact of tandem-flapping wings at a larger scale and higher reduced frequencies. The present research aims at analyzing the aerodynamic phenomena that take place for larger Reynolds numbers ($O(5 \times 10^4)$) at moderate reduced frequency (~ 1). This will be done through the design of a medium-scale tandem flapping wing system called the MechaRaptor. This system's region of interest is shown in Fig. 1, which plots the Reynolds number against the reduced frequency for a number of biological and mechanical flyers. The present paper covers the first stage (prototyping and preliminary results) of this experimental study. Tests results are presented in the range of Reynolds numbers and reduced frequencies commonly used for other mechanical fliers ($k \sim [0.02 - 0.2]$ and $Re \sim [3 \times 10^3 - 3 \times 10^4]$).

The aerodynamics of tandem wing systems are of interest in all Reynolds number ranges. Indeed, as it has already been demonstrated for steady configurations, the relative position of the two sets of wings can have a significant impact on the aerodynamic loads acting on the system [9]. The idea is therefore to determine if there are some attitude parameters that can be coupled in order to ensure the maximum efficiency for the whole system.

Finally, a better understanding of the flapping kinematics of tandem wing systems could also provide interesting insight for paleo-biologists. According to recent findings, the earliest flying animals may have been four-winged [10, 11]. As none of these species has survived, it seems that there was an obvious biological incentive to shift to two-winged flight instead. A better understanding of the aerodynamic properties of tandem wing flapping bodies may therefore shed some light on the evolution of animal flight.

*Ph.D. Student, Aerospace and Mechanical Engineering Department, University of Liège, Quartier Polytech, Allée de la découverte 9, 4000 Liège, Belgium, AIAA Student Member. t.lambert@uliege.be

†Associate Professor, Aerospace and Mechanical Engineering Department, University of Liège, Quartier Polytech, Allée de la découverte 9, 4000 Liège, Belgium, AIAA Senior Member.

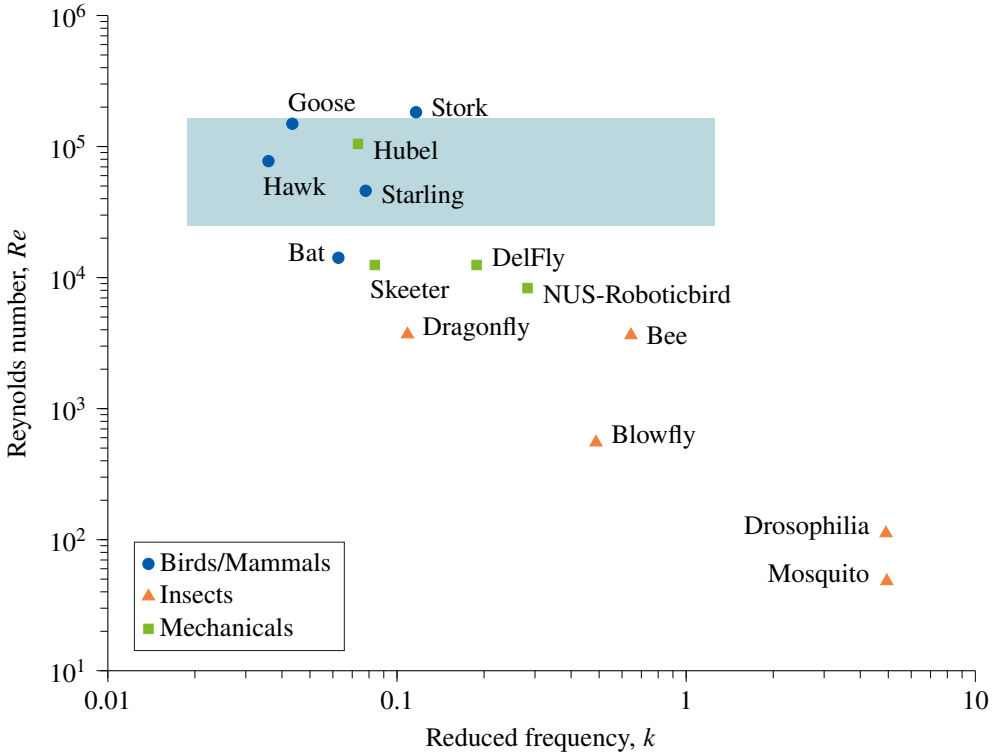

Fig. 1 Relationship of Reynolds number and reduced frequency for various animals and mechanical systems. The grey rectangle indicates the range of interest for the MechaRaptor. Adapted from [8].

A. Non-dimensional parameters

In order to better understand and compare the results obtained for different flight parameters, it is important to define dimensionless numbers. Besides the Reynolds number, the two most important parameters for flapping flight analysis are the *reduced frequency* and the *Strouhal number*.

1. Reduced frequency

The reduced frequency is one of the most important parameters in unsteady aerodynamics. This quantity represents the degree of unsteadiness of the flow:

$$k = \frac{\pi f c}{V_\infty} \tag{1}$$

where k is the reduced frequency, f is the wingbeat frequency, c is the wing chord and V_∞ is the freestream velocity. As the same wings are for all tests presented in the present paper, this reduced frequency can only be modified by changing the flapping frequency or the air speed.

According to Ames *et al.* [12], the reduced frequency can be used to differentiate flows based on their (un)steadiness. Following this, we can distinguish three regimes:

- Quasi-steady: $0 < k < 0.03$. Wakes effects are not very significant.
- Quasi-unsteady: $0.03 < k < 1$. Wake effect are significant but added-mass effects are not very important.
- Fully unsteady: $k > 1$. Flow is dominated by added-mass effects.

As shown in Fig. 1, the fully-unsteady region is often only observed for very small insects. Most animals and many mechanical flappers operate in the quasi-unsteady flow regimes. The MechaRaptor setup follows this trend by operating for the most part at reduced frequencies between 0.02 and 1.

2. Strouhal number

In flapping wing aerodynamics, the Strouhal number characterises the vortex shedding dynamics in the wake of the flapping wings. It is thus defined as

$$St = \frac{f A}{V_\infty} \tag{2}$$

where A is the flapping amplitude. According to Nudds *et al.* [13], the optimal propulsive efficiency for bird flight is obtained when $0.2 < St < 0.4$. The MechaRaptor will be analyzed for St between 0.03 and 0.5, in order to cover this optimal propulsive range.

B. Previous work

The present study is a continuation of a previous experiment study of a steady tandem wing system [9]. One of the main outcomes of this work was to show that the lift of the overall system was negatively impacted as the two sets of wings were brought closer to each other. A second important observation was that the system benefited from a larger lift when the two sets of wings were placed at very different dihedral angles. This result suggested that a dynamic system should experience best results when the two wings are flapping out of phase.

II. Experimental setup

A. Wind tunnel

This research and the experiments were conducted in the large low-speed wind tunnel of the University of Liège in November 2022. The MechaRaptor experiments were conducted in the aeronautical engineering test sections, whose dimensions are $2 \times 1.5 \times 1.5$ m (width $\times$ height $\times$ length). While the facility is able to reach speeds up to 60 m/s, the tests were limited to 15 m/s in static conditions and 10 m/s in flapping conditions to match realistic applications for flappers of this size. Future testing sessions will be carried out at higher airspeeds in order to cover a wider range of reduced frequencies and Reynolds numbers.

B. Flapping wing model

The mechanical system designed for this study is composed of two completely independent sets of flapping wings. Each set is made of an electric motor, a gearbox/crank mechanism and two half-wings, as seen in Figure 2. The two modules are then placed on a rail inside a fairing to assemble the whole system. To clearly differentiate the performance of each module, each one is placed on a different 6-component load sensor (in blue on Fig. 2a). The two modules are therefore completely separated and independent from one another.

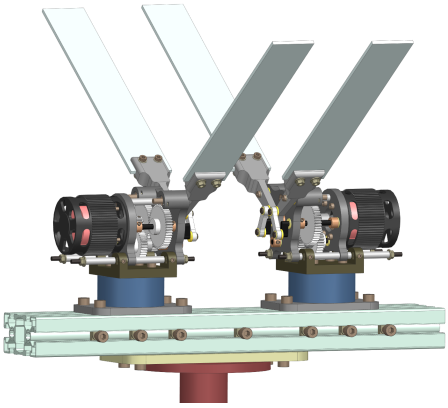

(a) Complete setup without fuselage.

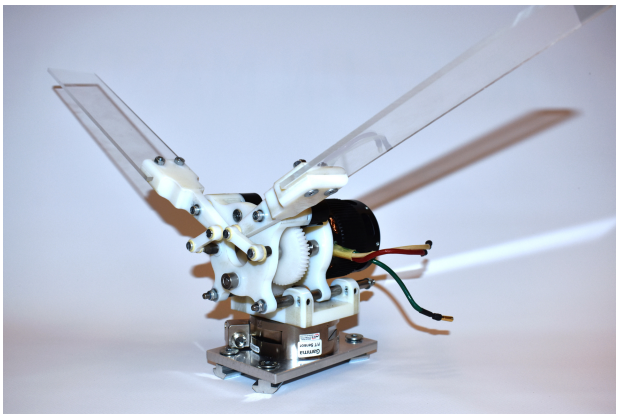

(b) Single isolated module.

Fig. 2 MechaRaptor base geometry.

The design of the mechanism focuses on modularity to accommodate a wide range of testing conditions. As such, the wing geometry (main dimensions, profile) and angles can be adapted easily without calling for major redesign of the

setup. One of the key aspect in tandem wing kinematics is the distance between the two sets of wings. To analyze this effect, the modules are placed on a rail that allows the precise setting of the horizontal distance between the front wing's trailing edge and the aft wing's leading edge.

Motor

Each module is powered by its own brushless DC motor (Plettenberg Advance 30). This very powerful (1.5 kW) motor was picked mostly to future-proof the test rig and allow the analysis of wings of different inertias without difficulty. Thanks to its active cooling, it will also allow testing at large flapping frequencies with less risks of overheating.

Gearbox and crank mechanism

As the motor operates at a high nominal velocity (6000 to 7000 RPM), a fair amount of reduction is required to attain the desired frequency. This is achieved using simple spur gears of appropriate size. A ratio of approximately 10:1 is thus applied between the motor shaft and the wing driver gears. This eventually leads to a nominal frequency of approximately 10 Hz for the MechaRaptor. Obviously, it is also possible to run the motor at a lower rate to achieve lower frequencies. However, the engine speed controller imposes a limiting bound to the rotation rate of the motor to prevent any damage. In the present setup, this lower limit is approximately equal to 900 RPM, which results in a minimum frequency of around 1.5 Hz.

The motion of the wings is imposed through a dual-crank mechanism. This improves the compactness of the modules, which allows the fuselage to be as narrow as possible. The dual-crank system also ensures a better symmetry in the motion of the two wings. Finally, since the crank is operating in the same plane as the flapping arc, regular ball bearings can be used, which reduces the friction in comparison to transverse shafts. This dual-crank mechanism is designed as two four-bar linkages. Due to space constraints and minimum lever length, the wing-pivot point had to be shifted slightly from the vertical position of the driver shaft. This resulted in a non-symmetrical amplitude for the flapping motion. The flapping amplitude thus obtained was between $-12°$ and $38°$.

Wings

The goal of this first study is to gain a deeper knowledge of the base aerodynamic phenomena. To reduce the number of design parameters, the first series of tests use simple uncambered wings (*i.e.*, rectangular flat plates). Each half-wing measures 0.2×0.05 m. In the present experiment, the wings are always fixed at $0°$ of angle of attack. Thanks to the modularity of the setup, more complex wing geometries (cambered wings, sweep, different pitch, etc.) will be studied in a second phase of the project.

The wings used for these simulations are made out of thick acrylic (PMMA) in order to guarantee rigidity and minimal deformation during the motion. More flexible wings will be used in the future to investigate the effect of flexibility on the aerodynamic loads.

The instantaneous flapping angles are measured using 12-bits magnetic rotary encoders (precision $\sim 0.08°$). For redundancy and reliability, each half-wing is equipped with one encoder. This also guarantees the proper assembly of the system and the symmetry between the two half-wings of each set.

Fuselage

The fuselage is kept as small as possible to prevent any major perturbation of the flow. One of the key elements for the fuselage is that it completely encases the modules alongside with their load sensors. As such, it shields the sensors from the flow, ensuring cleaner measurements and a better overall precision. The fuselage was printed in PLA in different parts than can be assembled around the main components of the system. Middle sections of different lengths were printed to accommodate the different horizontal distances between the two sets (see Fig. 3a).

C. Kinematics

As the goal of this first phase of the study is to understand the basic physics of the flow, the model will only undergo pure flapping motion (*i.e.*, no active pitching during the motion). The mechanism can then be kept simpler, more lightweight and more compact than active pitching devices.

In order to vary the operating conditions as much as possible, a sweep of frequencies from 1.5 to 3.5 Hz is carried out. Airspeeds of 0, 3, 5 and 8 m/s were tested at each frequency.

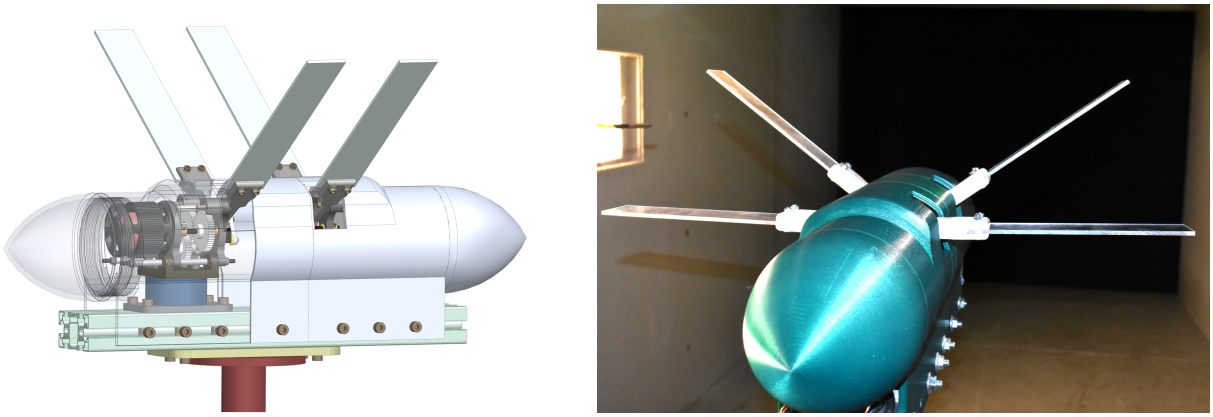

(a) CAD representation of the full system. **(b) Complete setup in the wind tunnel.**

Fig. 3 MECHARAPTOR complete setup.

Unfortunately, perfect synchronization of the two modules was found to be difficult to achieve. Analysis of the measurements of instantaneous angles reveals a frequency difference of approximately 0.5 % in average between the two sets over the full cycle (see Fig. 4). In addition, it was observed that the frequency was not rigorously constant during the entire test and some small oscillations were observed around the main frequency. This was likely caused by friction in the gearbox system and heating of the sleeve bearings that support the different shafts/axles. Although these frequency variations were not very significant in themselves, they led to loss of synchronization between the two modules and introduced phase differences.

In order to compare results properly and quantify the phase influence, each test is run for a significant amount of time (>200 periods). For each run, the phase difference is measured between the two sets of wings at every instant (based on the angle measurement). The forces are then averaged over a single period for any given phase offset.

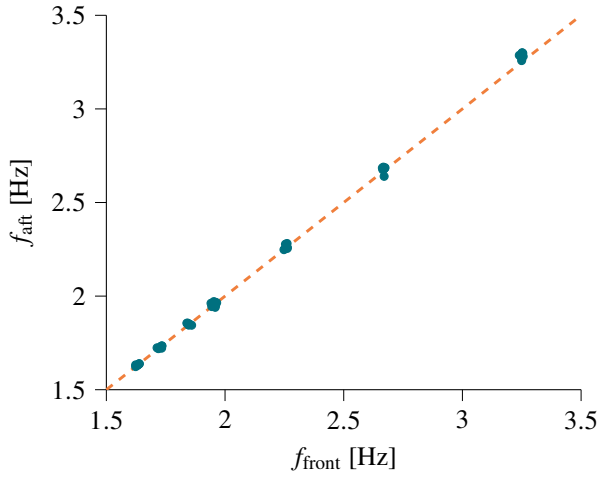

Fig. 4 Comparison of the frequency measured at each set in all test cases. Each individual point represents one experimental test case. Dashed line represents perfect match between the two frequencies.

III. Test results

A. Wind-off testing (inertia measurement)

In unsteady aerodynamics, the loads measured by the load sensors are a combination of aerodynamic, inertial and added mass effects. It is thus important to quantify the inertial and added mass contributions and subtract them from the

overall measurement in order to retrieve only the aerodynamic contribution.

For each test case (*i.e.*, each different separation distance between the wings and each different flapping frequency), the inertial contribution is measured by flapping the wings at wind-off conditions. Figure 5 plots the difference between the vertical forces measured at wind-off and wind-on conditions for one test case. It shows that the wind-on and wind-off load responses follow the same trends but the magnitudes of these loads are different.

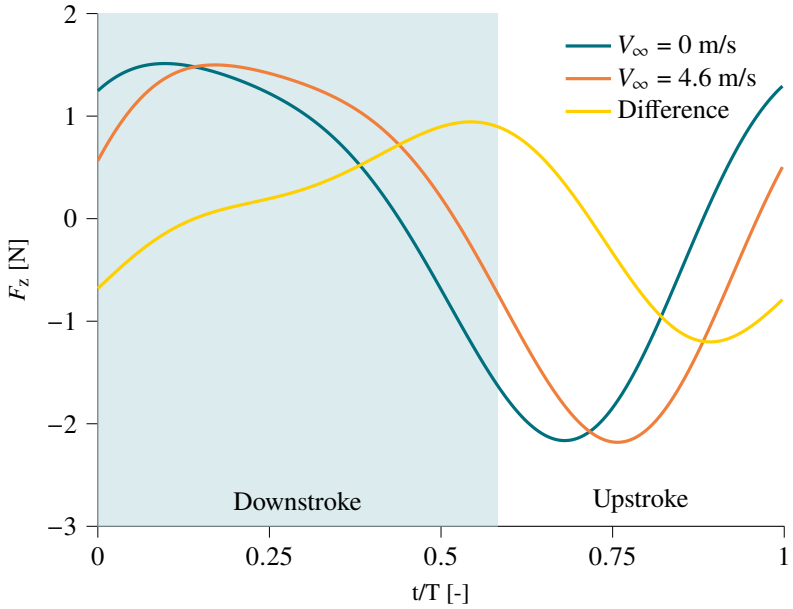

Fig. 5 Vertical force measured in wind-on and wind-off conditions and their difference. $D_x = 0.1\,m, f = 2.66\,Hz$ and $V_\infty = 4.6\,m/s$ ($k = 0.09$) .

The loads and load coefficients presented in the rest of this paper are all the *aerodynamic* ones (*i.e.*, the difference between the raw wind-on forces and the inertial wind-off contribution).

B. Wind-on testing

The results presented in the following sections are all formulated in terms of lift and drag coefficients (C_L and C_D). These are defined from the difference between the raw measured forces and the inertial forces as:

$$C_L = \frac{F_{z,\,\mathrm{tot}} - F_{z,\,\mathrm{wind\text{-}off}}}{0.5\rho V_\infty^2 A} \qquad C_D = \frac{F_{x,\,\mathrm{tot}} - F_{x,\,\mathrm{wind\text{-}off}}}{0.5\rho V_\infty^2 A} \tag{3}$$

where A is the total wing area per set ($= 0.02\,m^2$). For semi-flapping tests, the steady wing has obviously no inertial contribution. For all flapping wings, the load coefficients presented are cycle averages.

1. Semi-flapping

A first series of test was conducted by flapping only one module, while the other remained steady. Note that in order to compare results that are independent of the dihedral angles, the steady wing loads are normalized by taking into account the *projected* surface, A^*.

$$C_L^* = \frac{C_L}{\cos\Lambda} \qquad C_D^* = \frac{C_D}{\cos\Lambda} \tag{4}$$

where Λ is the dihedral angle.

As expected, the case where the first wing is steady and only the aft one flaps does not present any interesting results. The lift and drag of the front wing remain constant, irrespectively of the aft wing kinematics. The aft wing does not

seems to experience any noticeable impact either. Still, a more detailed study could be conducted in order to see if these observations remain true when the front wing is heavily separated for instance.

The most interesting case in semi-flapping is the one where the front wing flaps and the aft wing lays statically behind it at some fixed dihedral angle. Results for such a case are resented in Fig. 6. These results exhibit a very interesting phenomenon, which was not necessarily anticipated. The figure shows shows that the lift of the front wing is heavily impacted by the dihedral angle of the aft wing. A large reduction in lift is observed with increasing dihedral at all frequencies tested (1.25 and 2 Hz), for all horizontal spacings (0.03 and 0.05 m) and at all airspeeds (2.5, 4.6 and 7.7 m/s). The drag of the front wing on the other hand remains relatively stable.

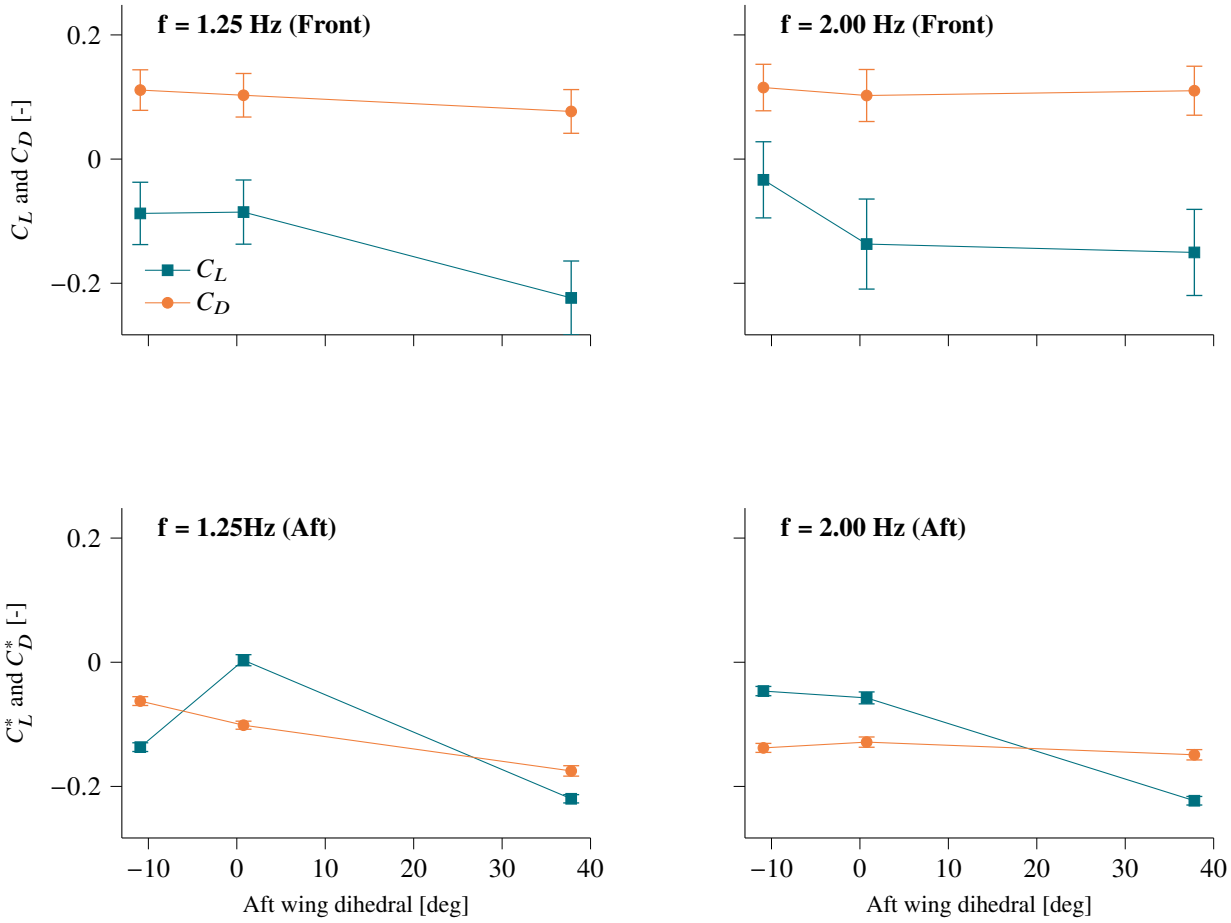

Fig. 6 Comparison of the lift and drag coefficient variation with the aft wing dihedral angle. D_x = 0.05 m and V_∞ = 7.7 m/s (k = 0.04 − 0.05).

As with the front wing, the lift of the aft wing decreases substantially with increasing dihedral angle. Figure 6 also shows that placing the aft wing at 0° of dihedral and lead to an increase in lift in some instances (f_{front} = 1.25 Hz) or remain relatively constant (f_{front} = 2.00 Hz). The same behavior was observed in the other test cases. However, this sharp lift increase is heavily linked to the reduced frequency and the horizontal distance between the two sets. This suggest that at some specific conditions, the interactions between the front wing's unsteady wake and the steady aft wing can benefit the entire system. An even more surprising observation is that in all test conditions, the aft wing seems to produce thrust. Further analysis should be carried on in order to explain this apparent thrust generation.

2. Tandem flapping

Tandem flapping tests were conducted at 7 different flapping frequencies and 3 different airspeeds (besides the wind-off tests). The tests were repeated for 3 different horizontal spacings (corresponding respectively to 0.6c, 1c and

2c).

Table 1 presents the various control parameters used for these experiments. Note that, as discussed in Section II.C, the true frequencies were not exactly the same as the ones presented in the table. The actual frequencies measured during the tests are the ones presented previously in Fig. 4.

Table 1 Settings for the flapping experiments.

Flapping frequencies	[Hz]	1.25, 1.5, 1.8, 2, 2.5, 3, 3.5
Airspeeds	[m/s]	2.5, 4.6, 7.7
Horizontal spacing	[m]	0.03, 0.05, 0.10

As explained previously, the aft wing is expected to be significantly impacted by the phase difference between the instantaneous flap angles of the two wings. Figure 7 shows the variation of cycle averaged lift and drag coefficients for each set of half-wings at different phase offsets. A first notable point is that for all phase differences, the first wing is the most important contributor to the overall lift of the system. In most instances, the aft wing is actually producing negative lift, which seriously impacts the overall performance. The mean drag is also lower for the aft wing in comparison to the one produced by the front one. This difference may be explained partially by a reduction of the induced drag component. The interaction with the fuselage may also result in an increase of the drag and the instabilities. A better characterisation of the flow field around the fuselage will be conducted at a later stage of the research to quantify this phenomenon more precisely.

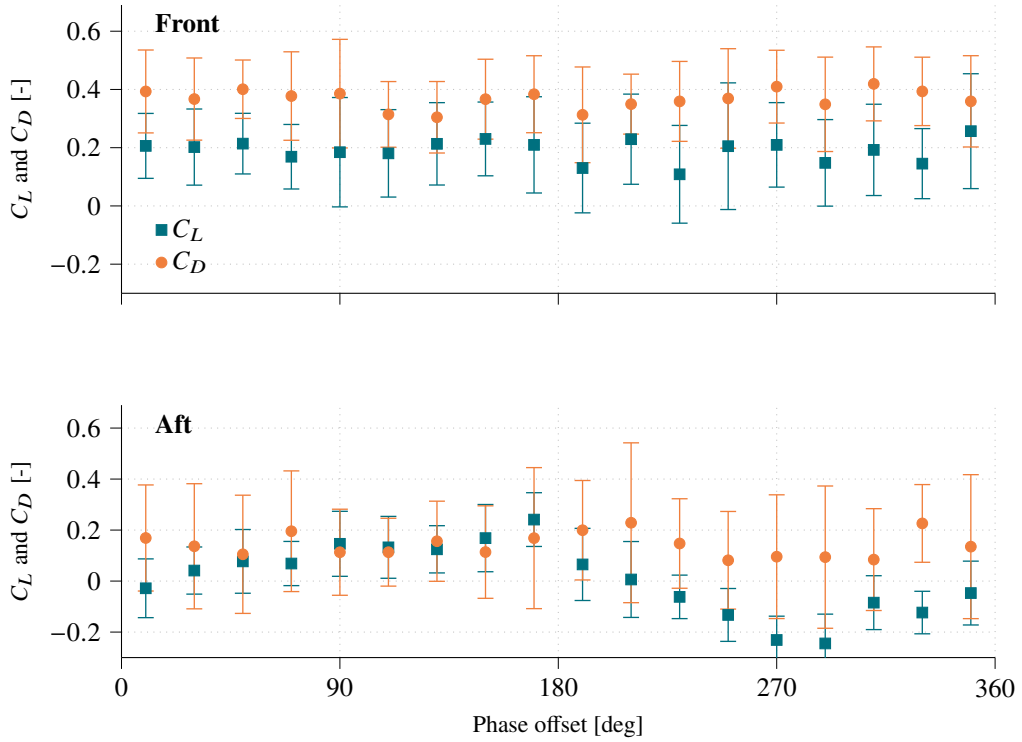

Fig. 7 Lift and drag coefficient variation with the phase difference between the two sets for the front and aft wings. A positive offset indicates that the front wing is leading the movement.
D_x = 0.03 m, f = 3.25 Hz and V_∞ = 4.6 m/s (k = 0.11) .

Figure 7 also shows that the phase difference plays a crucial role in the aerodynamic forces produced by the wings. In the situation depicted here ($D_x = 0.03$ m, $k = 0.11$) the aft wing experiences a significant loss of lift when the front

wing leads the motion by approximately 270 degrees. In contrast, when the two sets are completely out of phase (180° offset), the aft wing generates the most lift.

Perhaps more interestingly, the front wing is also impacted by the phase difference. Its lift appears to vary more or less as a mirror image of the lift of the aft wing. It is also worth noting that the drag of the front wing follows almost perfectly the variation of its lift. This suggests that drag variation with phase angle is mostly due to the induced drag contribution. This is not necessarily true for the aft wing. In that case, it is clear that the drag does not follows as closely the lift curve. Moreover, the standard deviation in the measurement data is much larger for the aft wing, which tends to hint at stronger instabilities in the flow. Viscous effects (separation, dynamic stall, wake interactions) seem to play a more important role on the aft wing.

It is interesting to note that, while the general behaviour is the same for most test conditions, the location of the optimum phase difference shifts with reduced frequency. This phenomenon is illustrated in Fig. 8. In this example, a lower lift is obtained when the front wing leads the aft wing by just a few degrees.

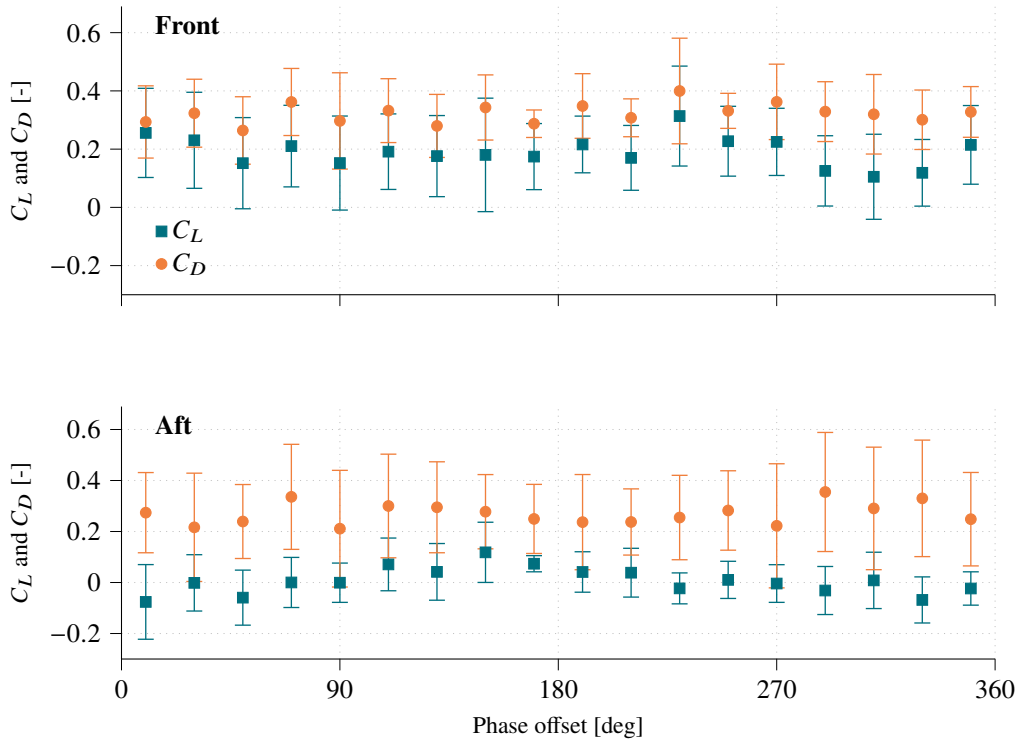

Fig. 8 Lift and drag coefficient variation with the phase difference between the two sets for the front (top) and aft (bottom) wings. A positive offset indicates that the front wings are leading the motion. $D_x = 0.03\,m$, $f = 2.67\,Hz$ and $V_\infty = 4.6\,m/s$ ($k = 0.09$) .

As shown by the static tests carried out in [9], the separation distance between the two modules plays an important role in the magnitude of the measured loads. Figure 9 presents the loads measured on the system when the horizontal distance between the two sets of wings is 0.1 m. These results should put in perspective with the ones presented in Fig 8, which present the exact same flow conditions, but with a spacing of 0.03 m. A first interesting observation is that the front wing's lift decreases when the horizontal distance is increased. The reduction in lift can be quantified to almost 50% in some cases. On the other hand, the drag of the front wing does not seems to be impacted in a meaningful way. For the aft wing, the lift remains relatively constant, irrespectively of the horizontal separation. It is however interesting to note that the phase offset that leads to a negative lift is shifted when the separation distance changes. A small reduction in the drag of the second wing is observed with the largest horizontal distance. This may be due to weaker tip vortices shed by the front wing.

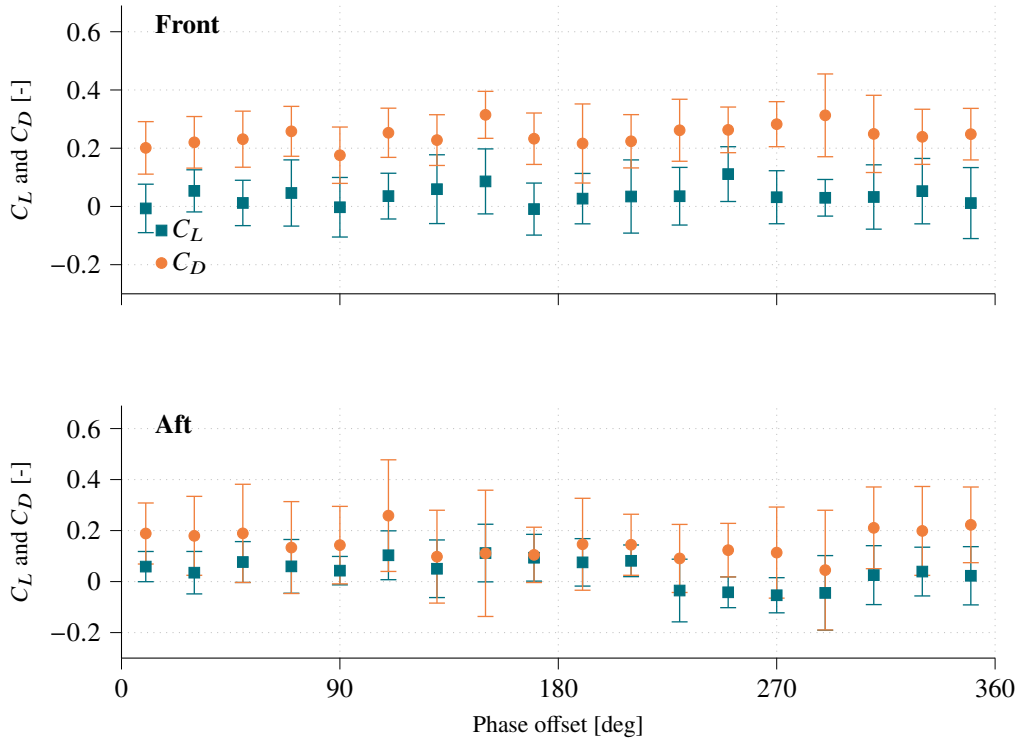

Fig. 9 Lift and drag coefficient variation with the phase difference between the two sets for the front (top) and aft (bottom) wings. A positive offset indicates that the front wings are leading the motion. $D_x = 0.10\,m$, $f = 2.66\,Hz$ and $V_\infty = 4.6\,m/s$ ($k = 0.09$) .

IV. Conclusions and future work

This paper presented the design and preliminary testing of a mechanical system able to flap a pair of tandem wing under various operating conditions and with different setup geometries. Preliminary results show a good behavior of the experimental setup and highlight interesting flow phenomena that will require more scrutiny at the next stages of the research.

The preliminary tests conducted in semi-flapping conditions (only one module active) already gave some valuable information. It was found that the front wing is heavily impacted by the presence of a steady aft wing. In all cases tested, the front wing experienced a significant reduction in lift when the front wing was placed at its maximum dihedral angle. Similarly, the aft wing itself was producing much less lift when it was in this same maximum dihedral angle. It was also observed that the aft wing produces thrust irrespectively of its dihedral angle.

For tandem flapping, the results presented here show a unambiguous influence of the phase difference between the instantaneous flap angles of the two wings on the lift and drag generated by each module. While the aft wing is the most impacted by this phase offset, some influence was also detected on the front wing. As expected, changes in reduced frequency or the separation distance were linked to a shift in the load response with respect to the phase offset. This is due to the geometry of the problem, as the position of the front wing's wake with respect to the aft wing is directly linked to these parameters. It was also clearly shown that the lift of the aft wing is always significantly lower than that of the front wing. Often, the aft wing does not generate mean lift at all, or worse, it generates a downforce. On the other hand, the drag of both sets of half-wings is of comparable magnitude. This suggests that the aft wing's drag is mostly due to viscous and friction effects. Finally, it was also demonstrated that the front wing's lift was significantly reduced when the separation distance between the two sets was increased.

The next phase of the research will focus on a more extensive test campaign, where the impact of all geometric and kinematics parameters will be quantified precisely.

Appendix

The entirety of this research is open-source. The CAD files, controller code, setup documentation, experimental data and the processing scripts are all available freely under the permissive MIT license. These materials can be found online at: `https://gitlab.uliege.be/mecharaptor`.

Acknowledgments

The authors would like to thank Antonio Martinez for his support, expertise and his watchmaker precision during the mechanical design of the MECHARAPTOR. We would also like to extend our most sincere gratitude to Quentin Grossman for his availability and help with the 3D printing pieces.

References

[1] Han, J., Hui, Z., Tian, F., and Chen, G., "Review on Bio-Inspired Flight Systems and Bionic Aerodynamics," *Chinese Journal of Aeronautics*, Vol. 34, No. 7, 2021, pp. 170–186. https://doi.org/10.1016/j.cja.2020.03.036.

[2] Keennon, M., Klingebiel, K., and Won, H., "Development of the Nano Hummingbird: A Tailless Flapping Wing Micro Air Vehicle," *50th AIAA Aerospace Sciences Meeting Including the New Horizons Forum and Aerospace Exposition*, American Institute of Aeronautics and Astronautics, Nashville, Tennessee, 2012, p. 588. https://doi.org/10.2514/6.2012-588.

[3] Nguyen, Q.-V., and Chan, W. L., "Development and Flight Performance of a Biologically-Inspired Tailless Flapping-Wing Micro Air Vehicle with Wing Stroke Plane Modulation," *Bioinspiration & Biomimetics*, Vol. 14, No. 1, 2018, p. 016015. https://doi.org/10.1088/1748-3190/aaefa0.

[4] Zyluk, A., Sibilski, K., and Czekalowski, P., "Experimental and Numerical Investigation of Entomopter Flapping Wings Aerodynamic Performance," *AIAA Atmospheric Flight Mechanics Conference*, American Institute of Aeronautics and Astronautics, Washington, D.C., 2016, p. 3543. https://doi.org/10.2514/6.2016-3543.

[5] Steltz, E., Avadhanula, S., and Fearing, R., "High Lift Force with 275 Hz Wing Beat in MFI," *2007 IEEE/RSJ International Conference on Intelligent Robots and Systems*, IEEE, San Diego, CA, USA, 2007, pp. 3987–3992. https://doi.org/10.1109/IROS.2007.4399068.

[6] Abdul Razak, N., Rothkegel, J. I., and Dimitriadis, G., "Experiments on a 3-D Flapping and Pitching Mechanical Model," *Proceedings of the 2009 International Forum on Aeroelasticity and Structural Dynamics*, IFASD, Dayton, Ohio, USA, 2009, p. 15.

[7] Abdul Razak, N., and Dimitriadis, G., "Wind Tunnel Experiments on a Flapping Drone," *Proceedings of the 15th International Forum on Aeroelasticity and Structural Dynamics, IFASD 2011*, IFASD, Paris, FR, 2011, p. 20.

[8] Hubel, T. Y., "Untersuchungen zur instationren Aerodynamik an einem vogelhnlichen Flgelschlagmodell." Ph.D. thesis, Technischen Hochschule Darmstadt, Darmstadt, DE, 2006.

[9] Lambert, T., Warbecq, N., Hendrick, P., Nudds, R., Andrianne, T., and Dimitriadis, G., "Numerical and Experimental Investigation of Tandem Wing Flyers," *AIAA Scitech 2019 Forum*, American Institute of Aeronautics and Astronautics, San Diego, California, 2019, p. 1620. https://doi.org/10.2514/6.2019-1620.

[10] Xu, X., Zhou, Z., Wang, X., Kuang, X., Zhang, F., and Du, X., "Four-Winged Dinosaurs from China," *Nature*, Vol. 421, No. 6921, 2003, pp. 335–340. https://doi.org/10.1038/nature01342.

[11] Dyke, G., de Kat, R., Palmer, C., van der Kindere, J., Naish, D., and Ganapathisubramani, B., "Aerodynamic Performance of the Feathered Dinosaur Microraptor and the Evolution of Feathered Flight," *Nature Communications*, Vol. 4, No. 1, 2013, p. 2489. https://doi.org/10.1038/ncomms3489.

[12] Ames, R., Wong, O., and Komerath, N., "On the Flowfield and Forces Generated by a Flapping Rectangular Wing at Low Reynolds Number," *Fixed and Flapping Wing Aerodynamics for Micro Air Vehicle Applications*, edited by T. J. Mueller, American Institute of Aeronautics and Astronautics, Reston ,VA, 2001, pp. 287–305. https://doi.org/10.2514/4.866654.

[13] Nudds, R. L., Taylor, G. K., and Thomas, A. L. R., "Tuning of Strouhal Number for High Propulsive Efficiency Accurately Predicts How Wingbeat Frequency and Stroke Amplitude Relate and Scale with Size and Flight Speed in Birds," *Proceedings of the Royal Society of London. Series B: Biological Sciences*, Vol. 271, No. 1552, 2004, pp. 2071–2076. https://doi.org/10.1098/rspb.2004.2838.